Pergamon

PII: S0301-9322(95)00072-9

Int. J. Multiphase Flow Vol. 23, No. 2, pp. 313–323, 1997

0301-9322/97 $17.00 + 0.00

FLOW OF SOLID–LIQUID MIXTURES IN INCLINED PIPES

P. DORON[1], M. SIMKHIS[2] and D. BARNEA[2]

[1]Environmental Sciences and Energy Research Department, Weizmann Institute of Science, Rehovot 76100, Israel

[2]Department of Fluid Mechanics and Heat Transfer, Tel-Aviv University, Tel-Aviv 69978, Israel

(Received 18 February 1996; in revised form 30 September 1996)

Abstract—The prediction of the flow characteristics of solid–liquid mixtures in inclined pipes has much practical importance, since long distance pipelines are bound to contain inclined sections. The three-layer model of Doron and Barnea (1993) was extended to account for the angle of inclination, which is expected to affect both the pressure drop and the limit deposit velocity. The extended model reproduces satisfactorily new experimental data as well as data of previous investigators. The additional effect of the gravitational force induces higher pressure gradients together with higher limit deposit velocity as the pipe's upward tilt is increased. For downwards inclination, the limit deposit velocity decreases drastically, and the pressure drop is reduced, since for downflow gravitation acts as a driving force. © 1997 Elsevier Science Ltd. All rights reserved.

Key Words: solid–liquid mixture, pipes, inclination, pressure drop

1. INTRODUCTION

The prediction of the flow characteristics in inclined pipes has much practical importance. When a long distance pipeline is constructed, topographic features of its course are bound to necessitate the construction of inclined sections, although the angles of inclination (especially upward grades) should be minimized. Cowper (1991) counted the upward slope restriction among the main guidelines for pipeline design, the limit being approx. 10–15% (5°–14°).

Both pressure drop and limit deposit velocity are expected to be affected significantly by the angle of inclination. However, building appropriate experimental facilities is very difficult, since long pipes are needed in order to investigate the fully developed flow. For this reason very few experimental data have been published to date (Shook and Roco 1991). Among these, one should note the work of Wilson and Tse (1984), and the experimental data on limit deposit velocity provided by Roco (1977) and Hashimoto *et al.* (1980). The difficulties in obtaining good reference data for pressure drop in inclined flow are exemplified by the work of Kao and Hwang (1979), where discrepancies between data in different figures are evident, probably due to misinterpretation of the components of the pressure drop.

This paper presents an extension of the three-layer model of Doron and Barnea (1993), originally applicable to horizontal flow, to account for pipe tilt. Following this the experimental facility of Tel-Aviv University was also modified in order to enable acquisition of data at inclinations of up to 7° upwards and downwards. The model results compare favorably with the new experimental data, as well as with the few sets of experimental data that have been found in the literature.

2. ANALYSIS

The three-layer model for solid–liquid flow in horizontal pipes presented by Doron and Barnea (1993) was modified to account for pipe inclination. Since the derivation of the model equations follows closely the model for horizontal pipes, it is reviewed briefly in the following section, with emphasis on the modifications related to pipe tilt.

Observations in our laboratory of the flow of solid–liquid mixtures at low flow rates indicate that while the upper strata of the bed may be moving, the lower strata may be stationary. Thus,

it is reasonable that at low bed velocities the particles at the bottom get 'stuck'. This leads to the description of the flow by means of a three-layer model, in which the bed is composed of two sub-layers: a stationary deposit at the bottom and a moving bed layer above it. The basic postulation is that the height of the stationary bed is such that the velocity of the moving bed above it is at a certain minimal value. This is the velocity which is required for the motion of the particles (i.e. the minimal velocity which causes 'stuck' particles to renew their motion). The upper portion of the pipe is occupied by a heterogeneous mixture.

2.1. *Minimal bed velocity*

The minimal bed velocity is obtained from the balance of driving and opposing torques acting on the solid particles in the lowermost stratum of the moving layer. A typical such particle, which rests in the 'trough' between adjacent particles of the upper part of the stationary bed and is at the verge of rolling, is shown schematically in figure 1. In this situation the driving torque (which arises from the drag exerted by the moving bed layer on the particle) and the opposing torque (which arises from the submerged weight of the particle and the moving bed particles, which lie on top of it) must balance.

The driving torque is $F_D L_D$, where F_D is the drag exerted by the surrounding medium (i.e. the moving bed layer), and L_D is the perpendicular distance from the center of rotation (O in figure 1), to the line of action of the driving force. The drag is found from

$$F_D = \tfrac{1}{2}\rho_L U_{bc}^2 C_D A_p \qquad [1]$$

where ρ_L is the density of the carrier liquid, U_{bc} is the minimal bed velocity, C_D is the drag coefficient for the particle, and A_p is the projection of the particle's exposed area on a plane normal to the flow direction. L_D passes through the centroid of A_p, hence

$$L_D = \frac{d_p}{2}\left(\sin\frac{\pi}{3} + 0.0137\right) \qquad [2]$$

where d_p is the particle's diameter.

The opposing torque is composed of the effect of the submerged weight of the particle ($W_p L_1$) and the effect of the solid particles in the moving bed layer pressing on it ($F_N L_2$).

The particle's submerged weight is

$$W_p = \tfrac{1}{6}\pi(\rho_S - \rho_L)g d_p^3 \qquad [3]$$

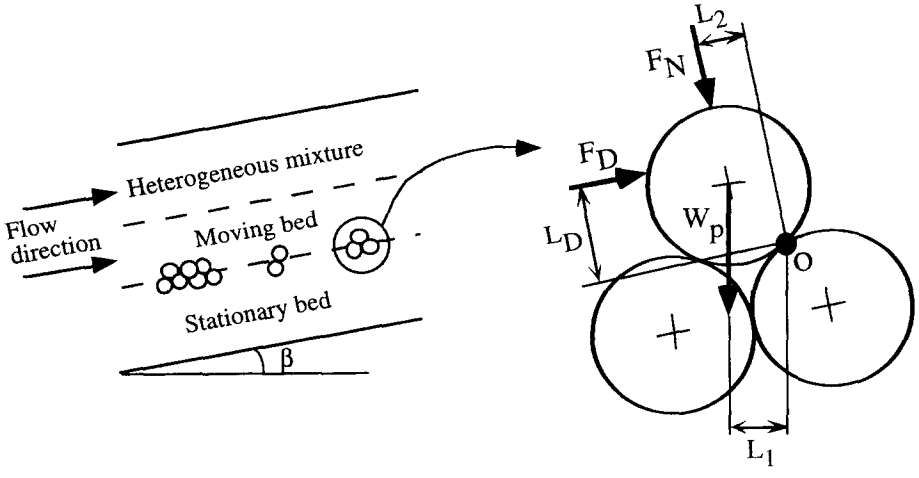

Figure 1. Schematic presentation of three-layer model and forces acting on a representative particle at the interface between the two bed layers.

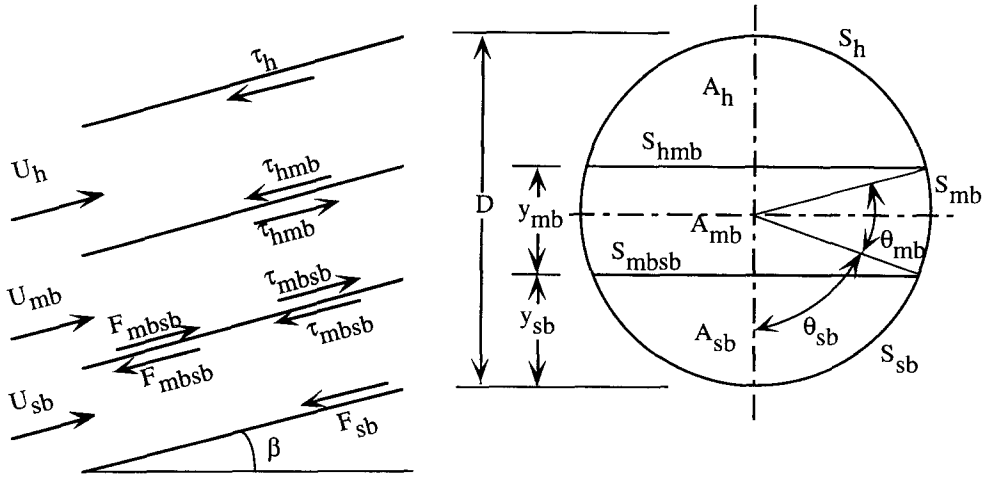

Figure 2. Three-layer model: geometry, velocities, shear stresses.

where ρ_S is the density of the solids, and g is the gravitational acceleration. The perpendicular distance from the line of action of this force to the center of rotation, 'O', is:

$$L_1 = \frac{d_p}{2}\sin\left(\frac{\pi}{6} + \beta\right) \qquad [4]$$

where β is the pipe's angle of inclination.

The normal force exerted by the column of particles lying above the particle under consideration is

$$F_N = W_p N \cos\beta = W_p C_{mb}\frac{y_{mb} - d_p}{d_p}\cos\beta \qquad [5]$$

where N is the average number of particles in the column, y_{mb} is the height of the moving bed layer, and C_{mb} is the moving bed concentration (assumed to be $C_{mb} = 0.52$, for cubic packing). The line of action passes through the center of the particle, hence

$$L_2 = \frac{d_p}{2}\sin\left(\frac{\pi}{6}\right) \qquad [6]$$

The minimal bed velocity it then extracted by equating the driving torque and the opposing torques

$$U_{bc} = \frac{\sqrt{1.559(\rho_S - \rho_L)g d_p\left[\sin\left(\frac{\pi}{6} + \beta\right) + \frac{\cos\beta}{2}C_{mb}\left(\frac{y_{mb}}{d_p} - 1\right)\right]}}{\rho_L C_D}. \qquad [7]$$

U_{bc} is the velocity of the moving bed in case of three-layer flow (namely, with a stationary layer at the bottom). When the mixture flow rate is increased, the height of the stationary bed diminishes, until it finally vanishes. From this point on, a further increase of the flow rate results in higher moving bed velocity.

2.2. The three-layer model

The whole flow is described by a three-layer model. Suppose that a solid–liquid mixture flows in a horizontal or slightly inclined pipe at a flow rate such that three layers exist in the pipe: a stationary bed at the bottom, a moving bed above it, and a heterogeneous mixture at the top (figure 2). Assuming uniform velocities in the three layers and constant layer thicknesses, one may now write the model equations. Only the main equations and the expressions affected by the pipe inclination are shown. Additional details can be found in Doron and Barnea (1993).

The continuity equation for the solid particles is

$$U_h C_h A_h + U_{mb} C_{mb} A_{mb} = U_s C_s A \quad [8]$$

and for the liquid phase

$$U_h(1 - C_h)A_h + U_{mb}(1 - C_{mb})A_{mb} = U_s(1 - C_s)A \quad [9]$$

where U is the mean axial velocity, C is the volumetric concentration of the solid particles and A is the pipe cross sectional area; the subscripts h and mb denote the heterogeneous upper layer and the moving bed layer, respectively; U_s is the superficial velocity of the mixture, C_s is the delivered concentration and A_h and A_{mb} are the cross sectional areas occupied by the dispersed layer and by the moving bed, respectively.

Force balances are written for the force components parallel to the mean flow velocity. The heterogeneous mixture in the upper dispersed layer is considered as a pseudo-liquid with effective properties. Hence

$$A_h \frac{dP}{dx} = -\tau_h S_h - \tau_{hmb} S_{hmb} - F_{hG} \quad [10]$$

where dP/dx is the pressure drop, τ_h and τ_{hmb} are the upper layer shear stress and the interfacial shear stress acting on the perimeters S_h and S_{hmb}, respectively, and F_{hG} is the gravitational force acting on the mixture in the upper layer (which is the only component affected by the pipe tilt)

$$F_{hG} = \rho_h g A_h \sin \beta \quad [11]$$

where ρ_h is the effective density in the heterogeneous layer.

For the moving bed layer the force balance yields

$$A_{mb} \frac{dP}{dx} = -F_{mbsb} - \tau_{mbsb} S_{mbsb} - F_{mb} - \tau_{mb} S_{mb} + \tau_{hmb} S_{hmb} - F_{mbG} \quad [12]$$

where F_{mbsb} is the Coulombic friction force acting at the interface betwen the moving bed and the stationary bed, S_{mbsb} (figure 2), τ_{mbsb} is the hydrodynamic shear stress acting on that interface; F_{mb} is the Coulombic friction force acting at the surface of contact of the moving bed with the pipe wall, S_{mb}, τ_{mb} is the hydrodynamic shear stress acting on that surface; and F_{mbG} is the gravitational force acting on the moving bed.

The Coulombic friction force is found by multiplying the normal force acting on a surface by the Coulombic friction coefficient, η. In the present case, the normal force consists of the contributions of the submerged weight of the solid particles, F_W, and of transmission of stress from the interface with the upper layer, F_ϕ. Thus, the friction force at the interface S_{mbsb} is

$$F_{mbsb} = F_{Wmbsb} + F_{\phi mbsb} \quad [13]$$

and at the pipe wall, S_{mb}

$$F_{mb} = F_{Wmb} + F_{\phi mb}. \quad [14]$$

The pipe inclination β only affects the submerged weight component. Hence

$$F_{Wmbsb} = \eta N_{mbsb} = \eta(\rho_S - \rho_L) g \cos \beta C_{mb} y_{mb} S_{mbsb} \quad [15]$$

and

$$F_{Wmb} = \eta N_{mb} = 2\eta(\rho_S - \rho_L) C_{mb} g \cos \beta R^2 \left[\left(\frac{y_{mb} + y_{sb}}{R} - 1 \right) \theta_{mb} + \cos(\theta_{sb} + \theta_{mb}) - \cos \theta_{sb} \right] \quad [16]$$

where R is the pipe's radius, y_{sb} is the stationary bed height, and θ_{mb} and θ_{sb} are the central angles to the edges of the moving bed and the stationary bed layers, respectively (figure 2).

The gravitational force acting on the moving bed layer in the direction parallel to the pipe axis

is

$$F_{mbG} = \rho_{mb} g A_{mb} \sin \beta \qquad [17]$$

where ρ_{mb} is the effective density of the moving bed.

The dispersion of the solid particles in the upper heterogeneous layer is assumed to be governed by the well-known diffusion equation

$$\epsilon \frac{d^2C}{dy^2} + w_y \frac{dC}{dy} = 0 \qquad [18]$$

where y is the vertical coordinate, perpendicular to the pipe axis, ϵ is the diffusion coefficient and w_y is the component of the hindered terminal velocity of the particles in the y direction ($w_y = w \cos \beta$). Taking the moving bed concentration, C_{mb}, as the boundary condition, the concentration profile in the upper layer is obtained

$$C(y) = C_{mb} e^{-w \cos \beta (y - y_{mb})/\epsilon}. \qquad [19]$$

Upon integration of [19] over the cross section of the upper layer, the equation for the mean concentration in that layer, C_h, is obtained

$$\frac{C_h}{C_{mb}} = \frac{2R^2}{A_h} \int_{\theta_{sb} + \theta_{mb}}^{\pi/2} e^{-\frac{w \cos \beta R}{\epsilon} [\sin \gamma - \sin(\theta_{sb} + \theta_{mb})]} \cos^2 \gamma \, d\gamma. \qquad [20]$$

The three-layer model is thus described by a set of six equations, [7]–[10], [12] and [20] for the six unknowns U_h (the mean velocity of the upper layer), U_{mb} (the mean velocity of the moving bed, which in the case of flow with a stationary bed is equal to the minimal possible moving bed velocity, U_{bc}), C_h (the mean concentration in the upper layer), y_{mb}, y_{sb} (the heights of the moving bed and of the stationary bed, respectively), and dP/dx (the pressure gradient). Additional expressions and constitutive relations required for closure of the equation set can be found in Doron and Barnea (1993). The model can also be used to predict the flow pattern transitions, as described in Doron and Barnea (1996).

3. EXPERIMENTAL FACILITY

The experimental system was originally constructed to obtain data on the characteristics of horizontal flow of solid–liquid mixtures. Detailed description of all the experimental facility's components can be found in Doron and Barnea (1995).

Several modifications were introduced to the test facility in order to obtain data for inclined flow. A schematic layout of the modified rig is presented in figure 3. The most important modification was reconstruction of the support system, such that the test section (7 in figure 3) can be tilted to angles of up to 7° from the horizontal, both up and down. The effect of inclination was found to be considerable even for these relatively small angles (which are due to limitations imposed by the physical size of the laboratory).

Some changes were made in order to improve the quality of the data at low flow rates, which correspond to flow with a stationary bed. The feed pipe (3 in figure 3) was reinstalled with a larger downward slope to prevent stationary bed build-up. A larger diameter sampling device (6 in figure 3) was installed, such that the concentration measurements at low flow rates and concentrations are more accurate. A variable-speed mixer was installed in the feed tank (1 in figure 3), which enables an easier and more accurate control of the delivered concentration (the suspension of particles in the tank, hence the delivered concentration, is controlled by the mixer rotational speed).

4. RESULTS

The additional effect of the gravitational force should result in a monotonous change of the pressure drop as the angle of inclination is increased. This is indeed evident in figure 4, which presents the dependence of the nondimensional pressure gradient, i (expressed in terms of meters of water per meter of pipe length) on the mixture velocity, U_s. The model results for flow with a

given delivered concentration at different inclinations are shown together with our experimental data. The pipe tilt affects the magnitude of the pressure drop, but the characteristic shape of the pressure drop curves is not changed. For very low flow rates, in the stationary bed flow pattern, the pressure drop varies little as the mixture velocity is changed. Note, that the acquisition of data for this flow pattern (which are scarce in the literature) was made possible by the modifications of the experimental rig. As the flow rate is increased, transition to flow with a moving bed occurs (namely, the limit deposit velocity is exceeded). A minimum in the pressure drop curve is encountered close to the limit deposit condition, followed by increasing pressure drop as the flow rate is increased further.

At positive grades the pressure drop increases as the inclination is increased. For downflow gravitation acts as a driving force, and for sufficiently steep slope it may suffice to induce flow. In that case i, which is the pressure drop applied by the pump, vanishes. However, if one imposes a lower flow rate than the one corresponding to the above equilibrium condition, then the pump actually induces an opposing force, indicated by a negative value of i. The magnitude of the negative pressure gradient increases as the downward slope is increased, since the driving effect of gravitation increases. For high velocities the pressure gradient is positive also for downflow, since the hydraulic friction resistance becomes increasingly large.

As reported previously for horizontal flow, higher delivered concentrations are associated with higher pressure drop for inclined pipes too. This is demonstrated in figure 5. For both positive and negative grades a higher solids content results in higher resistance to the flow (since a larger mean velocity is required in the suspended layer to enable suspension of a larger amount of particles).

Little data could be found in the literature on the pressure drop in inclined pipes. Figure 6 presents the effect of inclination on the pressure drop for operational conditions corresponding to those of Kao and Hwang (1979), $\rho_S = 2475$ kg/m^3, $d_p = 0.66$ mm, $D = 51$ mm, $C_s = 5.8\%$, but no quantitative comparison is possible because there are inconsistencies between different sets of data given in that paper. Nevertheless, qualitatively, the trend of the frictional pressure drop (which is obtained by subtracting the gravitational head from the total pressure drop, i.e. $i_f = i - \sin\beta$), is reproduced by the model. At low upward inclinations, the frictional pressure drop increases with β, whereas at higher inclinations, it reaches a maximum and then decreases very slowly. Comparison of the curves of the total pressure drop and the frictional pressure drop reveals that at high inclinations the dominant effect is the gravitational one (since the total pressure drop

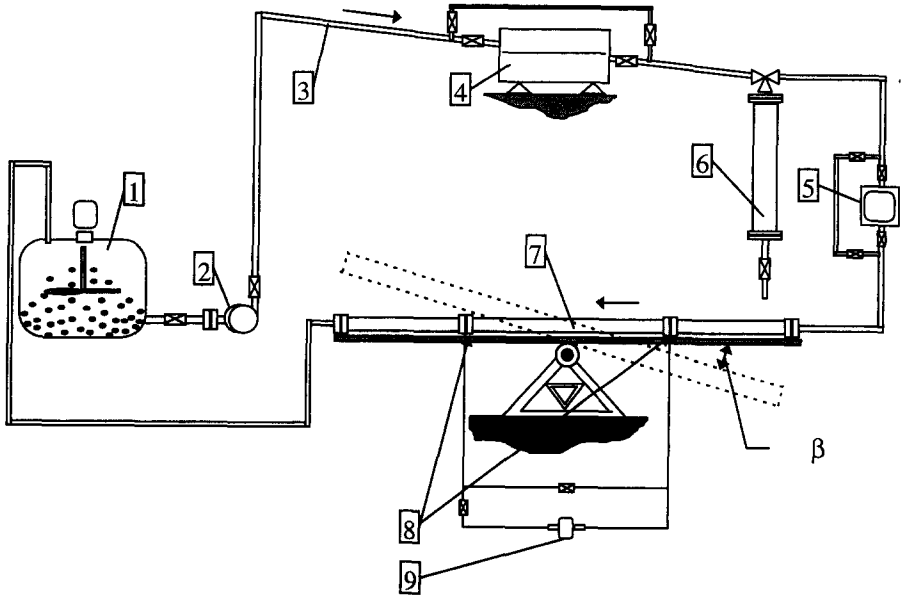

Figure 3. Layout of experimental system; (1) feed tank and mixer, (2) pump, (3) feed pipe, (4) mass flow meter, (5) volumetric flow meter, (6) sampling device, (7) test section, (8) pressure taps, (9) pressure transducer.

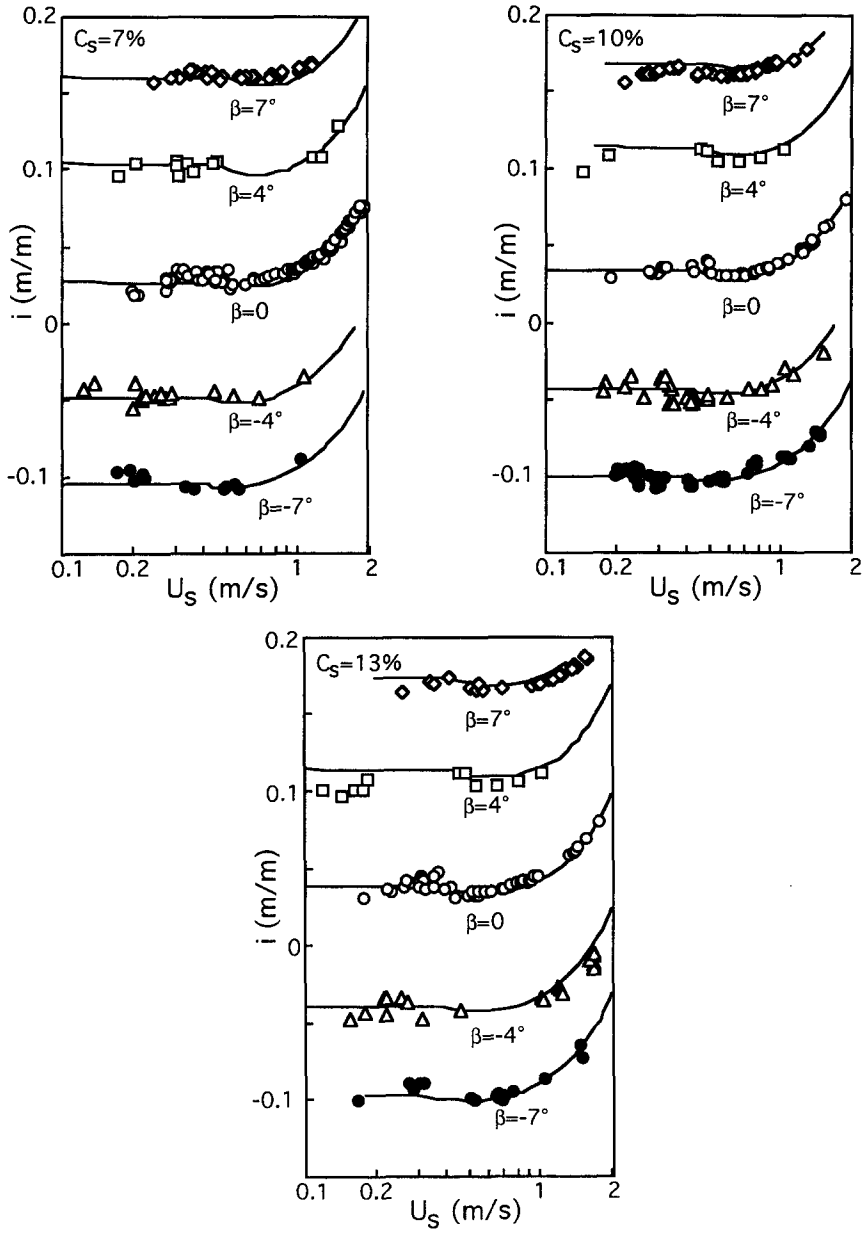

Figure 4. Effect of angle of inclination on pressure drop; $\rho_S = 1240$ kg/m^3, $d_p = 3$ mm, $D = 50$ mm. Symbols—data, lines—model.

increases despite the near constancy of the frictional contribution). This effect is independent of the flow pattern (at $U_s = 0.2$ m/s there is a stationary bed at all the inclinations considered, and at $U_s = 3$ m/s there is no stationary bed).

The effect of inclination on the limit deposit velocity, U_{LD}, is shown in figure 7. As one would expect, the stationary bed's range of existence is larger when the upward tilt is increased. This trend is indicated by both the model results and the experimental data. For downflow the model overpredicts the limit deposit velocity. One possible explanation is that the diffusion equation [18] does not fully incorporate the effect of the angle of inclination on the dispersion characteristics. For example, when considering vertical flow, it is obvious that the diffusion equation cannot explain the solids distribution in the pipe cross-section.

The minimal bed velocity, U_{bc}, depends on the angle of inclination, β, both explicitly and implicitly through the moving bed height, y_{mb} (see [7]). Intuition leads to believe that increasing

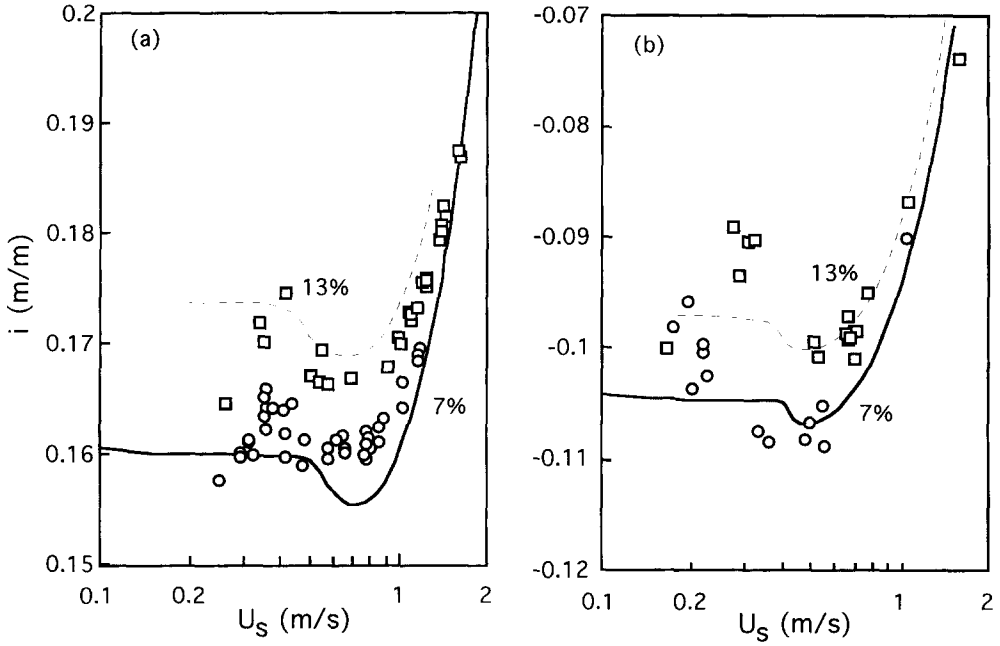

Figure 5. Effect of delivered concentration on pressure drop; (a) $\beta = -7°$, (b) $\beta = 7°$, $C_v = 7\%$: circles—data, solid line—model; $C_v = 13\%$: squares—data, dotted line—model. $\rho_S = 1240$ kg/m^3, $d_p = 3$ mm, $D = 50$ mm.

the upward inclination should induce a larger U_{bc}, hence a larger limit deposit velocity. Indeed, a higher upward slope requires a higher driving force for the particles, since the bed height should increase with β, as well as the distance to the line of action of the particle's weight, L_1, figure 1). On the other hand, the settling tendency of the particles decreases, as the effective settling velocity is $w \cos \beta$, which should reduce the bed height, since a larger portion of the solids can be transported in the upper layer for a given mixture flow rate (see [20]).

For the low range of upward tilt angles the first effect is dominant, as indicated by our experimental data and by other investigators, for example Wilson and Tse (1984). Their data for the flow of an aqueous mixture containing 1.1 mm diam. particles of density 2440 kg/m^3 in a 76 mm diam. pipe are presented in figure 8 together with our model predictions. The limit deposit condition is presented in terms of the Durand parameter F_L ($F_L = U_{LD}/\sqrt{2gD(\rho_S/\rho_L - 1)}$). The delivered

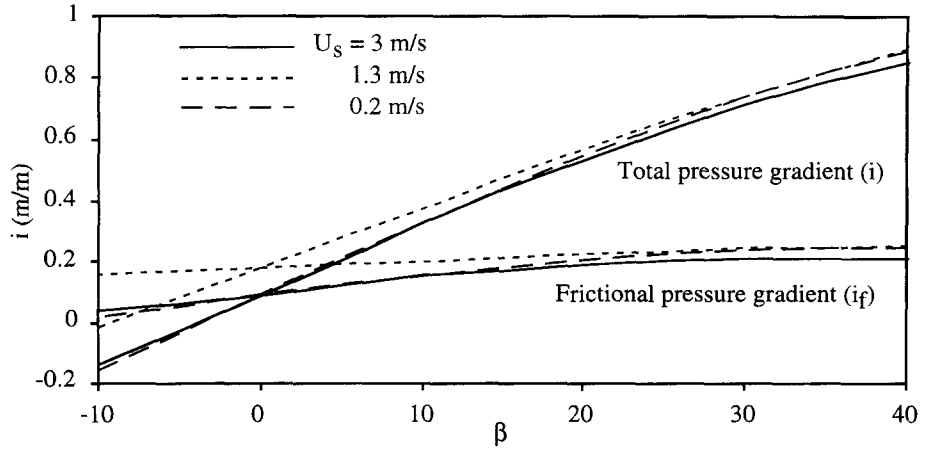

Figure 6. Effect of angle of inclination on the pressure drop, $\rho_S = 2475$ kg/m^3, $d_p = 0.66$ mm, $D = 51$ mm, $C_v = 5.8\%$.

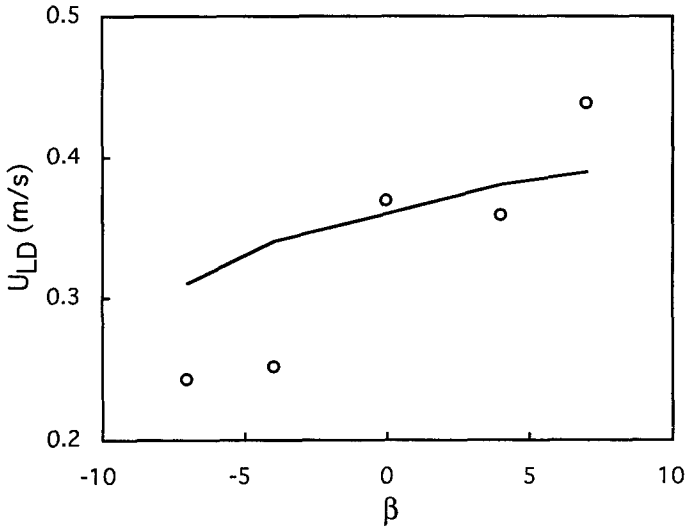

Figure 7. Effect of angle of inclination on limit deposit velocity; $\rho_S = 1240$ kg/m^3, $d_p = 3$ mm, $D = 50$ mm, $C_v = 13\%$. Circles—data, line—model.

concentration is not specified in this paper, and was estimated at 20%. The concentration affects the values of U_{LD}, but in any case, the trend predicted by the model conforms to the data.

At higher upward inclinations (around 20°–40°, depending on the operational conditions) the limit deposit velocity passes through a maximum and then decreases at a moderate rate. This is demonstrated in figure 9, where the data of Roco (1977) for water–sand ($\rho_S = 2650$ kg/m^3, $d_p = 0.36$ mm) mixture flow in a 100 mm pipe (as reported by Shook and Roco 1991) are presented together with the model results. The reverse trend is explained by the increased dominance of the settling velocity reduction as the inclination increases.

For downward inclinations the two effects described above are complimentary. When the pipe is inclined downwards, L_1 decreases with β. The effect on the settling tendency is the same as for upward flow. Thus, the limit deposit velocity diminishes drastically as the pipe is tilted downwards. Indeed, this has been noted by investigators such as Kao and Hwang (1979). In figure 9, the experimental data indicate a sharp decrease of U_{LD} for downwards inclinations. The extrapolation of the data, as presented by Roco (1977) shows that there is no stationary deposit at downward inclinations above approx. 15°–20°. The model also predicts a sharp reduction of U_{LD} when the magnitude of the downward inclination is larger than approx. 8°–10°. For large downwards inclinations ($\beta < -30°$) the weight of the particle constitutes a driving force, hence, no stationary bed can be expected.

The adverse effects of the angle of inclination can also be detected in figure 10, where the effect

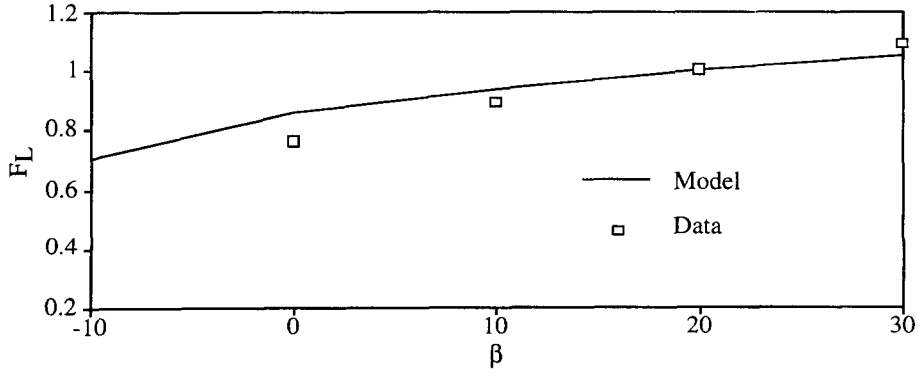

Figure 8. Effect of angle of inclination on Durand parameter—comparison of three-layer model results with Wilson and Tse's (1984) data, $\rho_S = 2440$ kg/m^3, $d_p = 1.1$ mm, $D = 76$ mm.

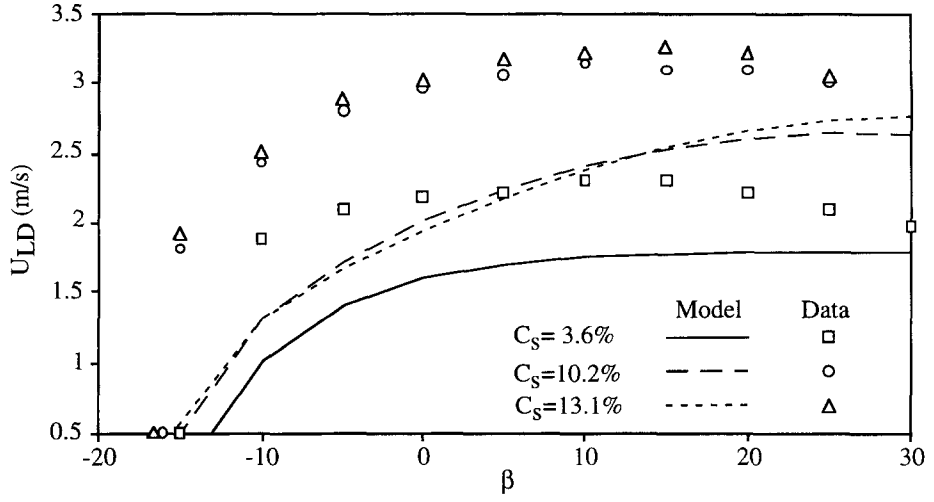

Figure 9. Effect of angle of inclination on limit deposit velocity—comparison of three-layer model results with Roco's (1977) data, $\rho_S = 2650$ kg/m^3, $d_p = 0.36$ mm, $D = 100$ mm.

of β on the predicted bed height is presented for a given set of operational conditions ($\rho_S = 2475$ kg/m^3, $d_p = 0.66$ mm, $D = 51$ mm, $U_s = 1.3$ m/s, $C_s = 5.8\%$). No data could be found regarding the bed height in inclined pipes, but one may expect the stationary bed height and the overall bed height to increase as the upward inclination is increased, since the gravitational effect becomes more pronounced. This is indeed evident from the model predictions for the lower positive slopes. However, a maximum is reached, and the bed height is reduced as the pipe is tilted further upwards. To explain this result one has to realize again that according to the three-layer model, the inclination has adverse effects for positive slopes and complimentary effects for negative slopes of the inclination.

5. SUMMARY

The three-layer model of Doron and Barnea (1993), originally developed for solid–liquid flow in horizontal pipes, was extended to account for pipe inclination. This was done mainly by inclusion of the gravitational effect in the force balances and modification of the principal directions in the diffusion equation.

New experimental data were used to validate the model results. The agreement between the data and the model regarding the pressure drop is satisfactory. However, the limit deposit velocity is overpredicted, indicating that the model provides an upper limit for the limit deposit condition (this holds also for the previous version of the model, see Doron and Barnea 1993).

The available data for pressure drop refer to inclinations of up to 7°. Indeed, it is reasonable

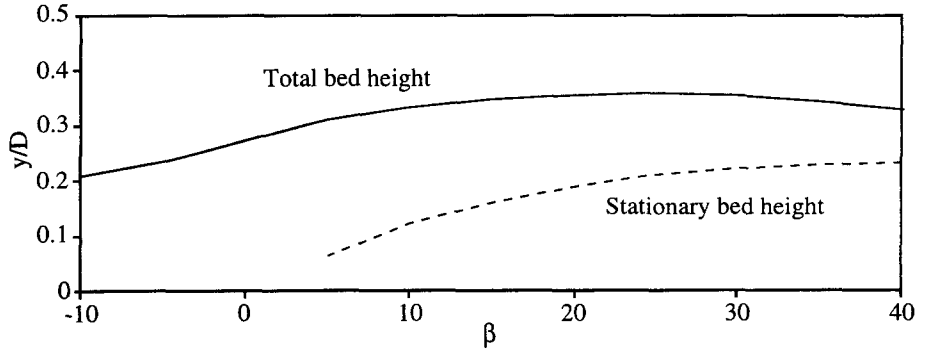

Figure 10. Effect of angle of inclination on the predicted bed height, $\rho_S = 2475$ kg/m^3, $d_p = 0.66$ mm, $D = 51$ mm, $U_s = 1.3$ m/s, $C_s = 5.8\%$.

that the basic assumptions of the model would not hold for nearly vertical flow. Therefore, application of the proposed model should be limited to relatively small angles of inclination.

REFERENCES

Cowper, N. T. (1991) Case studies of some major projects. In *Slurry Handling Design of Solid–Liquid Systems*, eds N. P. Brown and N. I. Heywood, pp. 625–652. Elsevier, London.

Doron, P. and Barnea D. (1996) Flow pattern maps for solid–liquid flow in pipes. *Int. J. Multiphase Flow* **22,** 273–283.

Doron, P. and Barnea, D. (1995) Pressure drop and limit deposit velocity for solid–liquid flow in pipes. *Chem. Engng Sci.* **50,** 1595–1604.

Doron, P. and Barnea, D. (1993) A three-layer model for solid–liquid flow in horizontal pipes. *Int. J. Multiphase Flow* **19,** 1029–1043.

Hashimoto, H., Noda, K., Masuyama, T. and Kawashima, T. (1980) Influence of pipe inclination on deposit velocity. In *Proc. of the 7th Int. Conf. on the Hydraulic Transport of Solids in Pipes*, Sendai, Japan, Paper F2, pp. 231–244.

Kao, D. T. Y. and Hwang, L. Y. (1979) Critical slope for slurry pipeline transporting coal and other solid particles. In *Proc. of the 6th Int. Conf. on the Hydraulic Transport of Solids in Pipes*, Canterbury, England, Paper A5, pp. 57–74.

Roco, M. C. (1977) Experimental investigation of critical velocity in pipelines for hydrotransport. *St. Cerc. Mec. Appl.* **36,** 111–112.

Shook, C. A. and Roco, M. C. (1991) *Slurry Flow: Principles and Practice*. Butterworth-Heinemann, Boston, MA.

Wilson, K. C. and Tse, J. K. P. (1984) Deposition limit for coarse particle transport in inclined pipes. In *Proc. of the 9th Int. Conf. on the Hydraulic Transport of Solids in Pipes*, Rome, Italy, Paper D1, pp. 149–161.